Electrophoresis of a Colloidal Sphere in a Circular Cylindrical Pore

Huan J. Keh and Jinn Y. Chiou
Dept. of Chemical Engineering, National Taiwan University, Taipei 106-17 Taiwan, R.O.C.

The electrophoretic motion of a dielectric sphere along the centerline of a long circular cylindrical pore is studied theoretically. The imposed electric field is constant and parallel to the nonconducting pore wall, and the particle and wall surfaces are assumed uniformly charged. Electrical double layers adjacent to solid surfaces are assumed to be thinner than particle radius and gap width between surfaces. The presence of the pore wall affects particle velocity: 1. an electroosmotic flow of the suspending fluid exists due to interaction between the electric field and the charged wall; 2. the local electric field on the particle surface is enhanced by the insulated wall, speeding up the particle; and 3. the wall increases viscous retardation of the moving particle. To solve electrostatic and hydrodynamic governing equations, general solutions are constructed from fundamental solutions in both cylindrical and spherical coordinate systems. Boundary conditions are enforced at the pore wall by Fourier transforms and then on the particle surface by a collocation technique. Typical electric-field-line, equipotential-line and streamline patterns for the fluid phase are exhibited, and corrections to the Smoluchowski equation for particle electrophoretic velocity are presented for various relative separation distances between the particle and wall. The presence of the pore wall always reduces the electrophoretic velocity; however, the net wall effect is quite weak, even for very small gap width between the particle and wall.

Introduction

Electrophoresis refers to the motion of a charged particle in an electrolyte solution when an electric field is applied, and has long been used as an effective technique for separation and identification of biologically-active compounds in the biochemical and clinical fields. It is well-known that a uniformly charged nonconducting particle of arbitrary shape undergoing electrophoresis migrates in an unbounded fluid with a velocity U_0 given by Smoluchowski's equation

$$U_0 = \frac{\epsilon\zeta}{4\pi\eta} E_\infty \tag{1}$$

provided that the local radii of curvature of the particle are much larger than the thickness of the electrical double layer surrounding the particle and that the imposed electric field E_∞ is constant (Morrison, 1970; Anderson, 1989). In this equation, ζ is the zeta potential associated with the particle surface, η is the fluid viscosity and $\epsilon/4\pi$ is the fluid permittivity. There is no rotational motion of the particle.

In addition to the particle movement, the interaction between the electric field and the ions within the mobile portion of the double layer generates a reverse tangential velocity for the fluid within the diffuse layer. This "slip velocity" at each point on the surface (or more precisely, on the outer edge of the diffuse layer), relative to the frame of the particle, is given by the Helmholtz expression for the electroosmotic flow

$$v_s = -\frac{\epsilon\zeta}{4\pi\eta} E_s. \tag{2}$$

Here, E_s is the local electric field which has no normal component for a nonconducting surface with a thin double layer. For a dielectric sphere of radius a, analytical studies (O'Brien and Ward, 1988; Hunter, 1989) show that the thin double

Correspondence concerning this article should be addressed to H. J. Keh.

layer approximation is accurate and Eqs. 1 and 2 are valid when

$$(\kappa a)^{-1}\exp\left(\frac{e|Z\zeta|}{2kT}\right) \ll 1 \tag{3}$$

where κ^{-1} is the Debye screening length characterizing the thickness of the double layer, Z is the valency of the most highly charged counterions in the fluid, e is the charge of a proton, k is Boltzmann's constant, and T is the absolute temperature.

In many electrophoresis applications to particle analysis or separation, natural convection of the suspending fluid due to Joule heating and nonuniform heat transfer creates problems. The generated heat may also cause the denaturation of heat-sensitive, biologically-active compounds. To avoid this unwanted mix-up, porous media such as polyacrylamide gels are often used to contain the suspension. Microporous gels or membranes could even be used to achieve high electric fields and permit separations based on both the size and the charge of particles (Jorgenson, 1986). In capillary electrophoresis, gels in the capillary column can minimize the particle diffusion, prevent the particle adsorption to the capillary walls, and eliminate electroosmosis, while serving as the anticonvective media (Ewing et al., 1989). Deep electrophoretic penetration and deposition of inert colloidal particles over the interstitial surfaces of porous composites has been suggested in the aerospace industry to protect the composites from burning or deterioration (Haber and Gal-Or, 1992). Other examples of electrophoresis with a bounded environment were given by Keh and Anderson (1985) and Zydney (1995). In all such systems, the Smoluchowski equation may no longer be applicable and one must determine how the nearby boundaries affect the movement of the particles.

During the past decade, much progress has been made in the theoretical development concerning electrophoresis of dielectric spheres in a variety of bounded systems. Using a method of reflections, Keh and Anderson (1985) analyzed the electrophoretic motions of a sphere normal to a large conducting plane, parallel to a large dielectric plane, along the axis of a long circular tube and along the centerline between two large parallel plates. The particle mobility for each case was determined in a power series of λ up to $O(\lambda^6)$, where the parameter λ is the ratio of the sphere radius to the distance between the sphere center and the boundary. It was found that the electrophoretic velocity of the particle is reduced (as a monotonic decreasing function of λ) compared to that for an unbounded case. The leading boundary effect is $O(\lambda^3)$, which is much weaker than the $O(\lambda)$ effect for a corresponding sedimentation problem.

Through an exact representation in spherical bipolar coordinates, numerical solutions for the electrophoretic velocity of a sphere in the vicinity of an infinite plane wall have also been obtained in two principal cases: the migration perpendicular to a conducting plane (Morrison and Stukel, 1970; Keh and Lien, 1991) and the movement parallel to an insulating wall (Keh and Chen, 1988). These results were in good agreement with the reflection analysis developed by Keh and Anderson (1985) when $\lambda < 0.7$. An interesting finding of the boundary effects is that the electrophoretic mobility of a sphere translating parallel to an insulating wall decreases, reaches a minimum (at $\lambda \approx 0.77$), and then increases as λ approaches unity. The particle velocity for the case $\lambda = 0.995$ can be as much as 23% higher than the value it would have in an unbounded system, subject to the constraint that the double-layer thickness remains small compared to the distance between the particle surface and the plane wall. An explanation of this enhancement of the particle velocity by the plane wall is that the driving force on the particle surface is increased enough due to the strong deformation of the electric field in the narrow gap region to more than compensate for the large viscous drag of the wall. Subsequently, the boundary effects on the electrophoresis of a sphere have also been investigated for geometries like migration along the axis of a circular orifice or disk (Keh and Lien, 1991) and motion in a concentric spherical cavity (Zydney, 1995).

The objective of this article is to obtain an exact solution for the electrophoretic motion of a colloidal sphere along the centerline of a long, circular cylindrical pore. Both the particle surface and the pore wall are assumed to be insulated. Thus, the axial conduction around the particle will generate large potential gradients on the particle surface. These gradients enhance the electrophoretic velocity, although their action will be retarded by the viscous interaction of the particle with the pore wall. Both the electrostatic enhancement and the hydrodynamic retardation increase as the ratio of particle-to-pore radii increases. Determining which effect is overriding at small particle-wall gap widths is a main target of this study.

Analysis

We consider the axisymmetric electrophoretic motion of a nonconducting sphere of radius a along the axis of a long circular cylindrical pore of radius b, as shown in Figure 1; the pore wall is also nonconducting. Here (ρ, ϕ, z) and (r, θ, ϕ) denote the cylindrical and spherical coordinates, respectively, and the origin of coordinates is chosen at the sphere center. The uniformly-applied electric field is expressed by $E_\infty \boldsymbol{e}_z$, where $\boldsymbol{e}_z$ is the unit vector in the z direction. The thickness of the electrical double layers adjacent to the solid surfaces is assumed to be small relative to the radius of the sphere and to the surface-to-surface spacing between the particle and the pore wall. Gravitational effects are ignored. The object is to determine the correction to the Smoluchowski equation (Eq. 1) for the particle due to the presence of the pore.

Before determining the electrophoretic velocity for the particle, the electrical potential and velocity fields in the fluid phase must be solved.

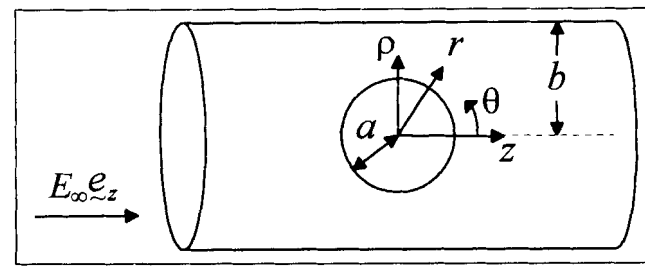

Figure 1. Electrophoresis of a spherical particle along the axis of an infinitely-long circular cylindrical pore.

Electrical potential distribution

The fluid outside the thin double layers is electrically neutral and is assumed to be of constant conductivity; hence, the electrical potential distribution $\Phi(x)$ is governed by Laplace's equation

$$\nabla^2\Phi = 0. \tag{4}$$

The local electric field $E(x)$ equals $-\nabla\Phi$. The potential gradient far from the particle approaches the undisturbed applied electric field and the normal component of the current flux at the surface of the insulating particle and pore wall vanishes. Thus, the electrical potential is subject to the following boundary conditions

$$e_r\cdot\nabla\Phi = 0 \qquad \text{at } r = a \tag{5a}$$

$$e_\rho\cdot\nabla\Phi = 0 \qquad \text{at } \rho = b \tag{5b}$$

$$\Phi \to -E_\infty z \qquad \text{as } |z| \to \infty \tag{5c}$$

where e_r and e_ρ are the unit vectors in the r and ρ directions. The undisturbed potential at the plane $z = 0$ has been set equal to zero for convenience.

Since the governing equation and boundary conditions are linear, one can write the potential distribution Φ, which is antisymmetric with respect to z, as the superposition

$$\Phi = \Phi_w + \Phi_s. \tag{6}$$

Here, Φ_w is a Fourier-Bessel integral solution of Eq. 4 in cylindrical coordinates that represents the disturbance produced by the pore wall plus the undisturbed electrical potential and is given by

$$\Phi_w = -E_\infty z + E_\infty\int_0^\infty R(\omega)I_0(\omega\rho)\sin(\omega z)d\omega \tag{7}$$

where I_0 is the modified Bessel function of the first kind of order zero and $R(\omega)$ is an unknown function of ω. The second term on the righthand side of Eq. 6, Φ_s, is a solution of Eq. 4 in spherical coordinates representing the disturbance generated by the sphere and is given by an infinite series in harmonics

$$\Phi_s = E_\infty\sum_{m=1}^{\infty} T_m r^{-(m+1)}P_m(\cos\theta) \qquad (m \text{ is odd}) \tag{8}$$

where P_m is the Legendre polynomial of order m and T_m are unknown constants. Note that a solution of Φ of the form given by Eqs. 6–8 immediately satisfies boundary conditions in Eq. 5c.

A brief conceptual description of the solution procedure to determine $R(\omega)$ and T_m is given below to help follow the mathematical development. At first, boundary condition (Eq. 5b) is exactly satisfied on the pore wall by using a Fourier sine transform. This permits the unknown function $R(\omega)$ to be determined in terms of the coefficients T_m. Then, the boundary condition in Eq. 5a on the surface of the sphere can be satisfied by making use of the collocation method, and the solution of the collocation matrix provides numerical values for the coefficients T_m.

Substitution of the solution Φ given by Eqs. 6–8 into the boundary condition of Eq. 5b and application of the Fourier sine inversion on the variable z lead to a solution for $R(\omega)$ in terms of the coefficients T_m

$$R(\omega) = \sum_{m=1}^{\infty} T_m(-1)^{(m-1)/2}\left(\frac{2\omega^m}{\pi m!}\right)\frac{K_1(b\omega)}{I_1(b\omega)} \qquad (m \text{ is odd}) \tag{9}$$

where I_1 and K_1 are the modified Bessel functions of the first and second kinds, respectively, of order one. Utilizing the relation

$$\frac{\partial}{\partial r} = \sin\theta\frac{\partial}{\partial\rho} + \cos\theta\frac{\partial}{\partial z} \tag{10}$$

one can apply boundary condition of Eq. 5a to Eqs. 6–8 after the substitution of Eq. 9 to yield

$$\sum_{m=1}^{\infty} T_m\alpha_m(a,\theta) = \cos\theta \qquad (m \text{ is odd}), \tag{11}$$

where

$$\alpha_m(r,\theta) = (-1)^{(m-1)/2}\frac{2}{\pi m!}\int_0^\infty \omega^{m+1}\frac{K_1(b\omega)}{I_1(b\omega)} \times[I_1(\omega r\sin\theta)\sin(\omega r\cos\theta)\sin\theta + I_o(\omega r\sin\theta)\cos(\omega r\cos\theta)\cos\theta]d\omega - (m+1)r^{-(m+2)}P_m(\cos\theta). \tag{12}$$

The definite integral in Eq. 12 must be performed numerically.

To satisfy the condition in Eq. 11 exactly along the entire surface of the sphere would require the solution of the entire infinite array of unknown constants T_m. However, the collocation technique (O'Brien, 1968; Leichtberg et al., 1976; Keh and Lien, 1991) enforces the boundary condition at a finite number of discrete points on the quarter-circular generating arc of the sphere (from $\theta = 0$ to $\theta = \pi/2$, owing to the geometrical symmetry) and truncates the infinite series in Eq. 8 into a finite one. If the spherical boundary is approximated by satisfying the condition of Eq. 5a at M discrete points on its generating arc, the infinite series in Eq. 8 is truncated after M terms, resulting in a system of M simultaneous linear algebraic equations in the truncated form of Eq. 11. This matrix equation can be solved to yield the unknown constants T_m required in the truncated form of Eqs. 6–9 for the electrical potential distribution. The accuracy of the truncation technique can be improved to any degree by taking a sufficiently large value of M. Naturally, as $M \to \infty$ the truncation error vanishes and the overall accuracy of the solution depends only upon the numerical integration required in evaluating the matrix elements.

In this subsection, the electrical potential field inside a cylindrical pore containing a colloidal sphere has been solved for the case that the thin double layers adjacent to the solid surfaces do not overlap with each other, and the potential distribution is caused by an axially-applied electric field disturbed by the presence of the sphere. For the situation that there is no external electric field and the double layers associated with the particle and pore wall may have arbitrary thickness, the electrostatic potential field was determined by Smith and Deen (1980, 1983) for both cases of constant surface charge densities and constant surface potentials using an approach similar to that used in this subsection.

Fluid velocity distribution

Having obtained a solution for the electrical potential distribution, we can now proceed to find the fluid velocity field. Because the Reynolds numbers of electrokinetic flows are small, the fluid motion outside the thin double layers is governed by the quasi-steady fourth-order differential equation for viscous axisymmetric creeping flows

$$E^2(E^2\Psi) = 0 \tag{13}$$

in which the Stokes stream function Ψ is related to the velocity components in cylindrical coordinates by

$$v_\rho = \frac{1}{\rho}\frac{\partial \Psi}{\partial z} \tag{14a}$$

$$v_z = -\frac{1}{\rho}\frac{\partial \Psi}{\partial \rho} \tag{14b}$$

and the Stokes operator E^2 has the form

$$E^2 = \rho\frac{\partial}{\partial \rho}\left(\frac{1}{\rho}\frac{\partial}{\partial \rho}\right) + \frac{\partial^2}{\partial z^2}.$$

Since the electric field acting on the diffuse ions within the double layer at each solid surface produces a relative tangential fluid velocity at the outer edge of the double layer as given by Eq. 2, the boundary conditions for the velocity field are

$$\boldsymbol{v} = U\boldsymbol{e}_z + \frac{\epsilon\zeta_p}{4\pi\eta}\nabla\Phi \qquad \text{at } r = a \tag{15a}$$

$$\boldsymbol{v} = \frac{\epsilon\zeta_w}{4\pi\eta}\nabla\Phi \qquad \text{at } \rho = b \tag{15b}$$

$$\boldsymbol{v} \to v_\infty \boldsymbol{e}_z \qquad \text{as } r \to \infty \tag{15c}$$

where $v_\infty = -\epsilon\zeta_w E_\infty/4\pi\eta$, which is the electroosmotic velocity caused by the interaction between the applied electric field and the pore wall in the absence of the particle; ζ_p and ζ_w are the zeta potentials of the particle and of the pore wall, respectively; U is the electrophoretic velocity of the particle to be determined. Note that the normal component of $\nabla\Phi$ vanishes at the solid surfaces as required by Eqs. 5a and 5b, and the position dependence of the tangential electric field is obtained from the potential distribution given by Eqs. 6–9 with coefficients determined from Eq. 11.

Because the particle is freely suspended in the fluid and the particle "surface" (the outer limit of the double layer) encloses a neutral body, the external field produces no net force on the particle. For the axisymmetric motion considered in this work, the sphere translates without rotation and one can evaluate U by satisfying the constraint of zero drag force after solving Eqs. 13 and 15.

In view of the linearity of the governing equation and boundary conditions, the total flow can be decomposed into two contributions. First, we consider the fluid motion about a sphere translating along the axis of a circular cylindrical pore with velocity $U\boldsymbol{e}_z$ and with no tangential electrokinetic velocity at the particle surface, while the pore wall and the fluid far from the particle are moving with a velocity equal to $v_\infty \boldsymbol{e}_z$. The boundary conditions for this subproblem are

$$\boldsymbol{v} = U\boldsymbol{e}_z \qquad \text{at } r = a \tag{16a}$$

$$\boldsymbol{v} = v_\infty \boldsymbol{e}_z \qquad \text{at } \rho = b \tag{16b}$$

$$\boldsymbol{v} \to v_\infty \boldsymbol{e}_z \qquad \text{as } r \to \infty. \tag{16c}$$

The Stokes equations for this flow were semianalytically solved by Haberman and Sayre (1958) and Leichtberg et al. (1976). They obtained the stream function (Ψ_1) for the flowing fluid and determined that the force exerted by the fluid on the particle can be written in the form

$$F_1 = -6\pi\eta a(U - v_\infty)\alpha \tag{17}$$

where α is the correction factor to Stokes' law due to the presence of the pore wall. The value of α depends upon the ratio a/b and can be numerically computed using the boundary collocation method. An approximate solution for α in a power series of a/b up to $O(a/b)^{10}$ has also been obtained (Happel and Brenner, 1983).

We now consider the fluid flow caused by a stationary sphere situated on the axis of a circular cylindrical pore with a tangential electrokinetic velocity at each solid surface; namely, the boundary conditions become

$$\boldsymbol{v} = \frac{\epsilon\zeta_p}{4\pi\eta}\nabla\Phi \qquad \text{at } r = a \tag{18a}$$

$$\boldsymbol{v} = \frac{\epsilon\zeta_w}{4\pi\eta}\nabla\Phi - v_\infty \boldsymbol{e}_z \qquad \text{at } \rho = b \tag{18b}$$

$$\boldsymbol{v} \to \boldsymbol{0} \qquad \text{as } r \to \infty. \tag{18c}$$

Superposition of this velocity field upon that formerly considered, caused by a sphere translating in the pore, yields the total fluid velocity field generated by the electrophoretic motion of a sphere along the axis of a circular cylindrical pore. By obtaining the force F_2 acting on the stationary sphere, adding it to F_1 given by Eq. 17 and equating the sum to zero, Smoluchowski's equation with the wall correction will result.

To find the drag force acting on the stationary sphere with a tangential velocity distribution at the surface, we express the stream function, which is symmetric about the plane $z = 0$, in the form

$$\Psi_2 = \Psi_w + \Psi_s. \tag{19}$$

Here Ψ_w is a solution of Eq. 13 in cylindrical coordinates that represents the disturbance produced by the pore wall and is given by a Fourier-Bessel integral

$$\Psi_w = \int_0^\infty [X(\omega)\rho I_1(\omega\rho) + Y(\omega)\rho^2 I_0(\omega\rho)]\cos(\omega z)d\omega \tag{20}$$

where $X(\omega)$ and $Y(\omega)$ are unknown functions of ω. The second part of Ψ_2, denoted by Ψ_s, is a solution of Eq. 13 in spherical coordinates representing the disturbance generated by the sphere and is given by

$$\Psi_s = \sum_{n=2}^{\infty} (B_n r^{-n+1} + D_n r^{-n+3}) G_n^{-1/2}(\cos\theta) \qquad (n \text{ is even}) \tag{21}$$

where $G_n^{-1/2}$ is the Gegenbauer polynomial of the first kind of order n and degree $-1/2$; B_n and D_n are unknown constants. Note that the boundary condition in Eq. 18c is immediately satisfied by a solution of the form given by Eqs. 19–21.

As was the case with the solution for the electrical potential distribution, the determination of $X(\omega)$, $Y(\omega)$, B_n and D_n will be undertaken by a two-step procedure. First, the boundary condition of Eq. 18b is exactly satisfied on the pore wall by a Fourier cosine transform; then, the condition in Eq. 18a is satisfied numerically at collocation points on the particle surface.

Application of the boundary condition of Eq. 18b to Eqs. 19–21 using Eqs. 6–9 and 14 leads to

$$\int_0^\infty \{X(\omega)\omega I_1(b\omega) + Y(\omega)b\omega I_0(b\omega)\}\sin(\omega z)d\omega = -\sum_{n=2}^{\infty} [B_n \beta_n^{(1)}(b,z) + D_n \beta_n^{(2)}(b,z)], \tag{22a}$$

$$\int_0^\infty \{X(\omega)\omega I_0(b\omega) + Y(\omega)[2I_0(b\omega) + b\omega I_1(b\omega)]\}\cos(\omega z)d\omega = -\sum_{n=2}^{\infty} [B_n \beta_n^{(3)}(b,z) + D_n \beta_n^{(4)}(b,z)], + \upsilon_\infty \sum_{m=1}^{\infty} T_m \beta_m^{(5)}(b,z), \tag{22b}$$

where m is odd, n is even, and functions $\beta_n^{(i)}(\rho, z)$ for $i = 1$, 2, 3, 4 and 5 are defined by Eqs. A1–A5 in the Appendix. By applying Fourier cosine integral inversions on the variable z to Eq. 22, one has

$$X(\omega)\omega I_1(b\omega) + Y(\omega)b\omega I_0(b\omega) = -\sum_{n=2}^{\infty} [B_n A_n^{(1)}(\omega) + D_n A_n^{(2)}(\omega)], \tag{23a}$$

$$X(\omega)\omega I_0(b\omega) + Y(\omega)[2I_0(b\omega) + b\omega I_1(b\omega)] = -\sum_{n=2}^{\infty} [B_n A_n^{(3)}(\omega) + D_n A_n^{(4)}(\omega)] + \upsilon_\infty \sum_{m=1}^{\infty} T_m A_m^{(5)}(\omega), \tag{23b}$$

where

$$A_n^{(i)}(\omega) = \begin{cases} \dfrac{2}{\pi}\displaystyle\int_0^\infty \beta_n^{(i)}(b,z)\sin(\omega z)dz & (i = 1,2) \\ \dfrac{2}{\pi}\displaystyle\int_0^\infty \beta_n^{(i)}(b,z)\cos(\omega z)dz & (i = 3,4,5) \end{cases}. \tag{24}$$

The closed forms of functions $A_n^{(i)}(\omega)$ after integration are given by Eqs. A6–A10.

Equations 23a and 23b are solved simultaneously for $X(\omega)$ and $Y(\omega)$. This solution is substituted back into Eqs. 19–21, leading to a new expression for the stream function Ψ_2 in terms of the unknown constants B_n and D_n. Presented below is the result for the velocity components

$$\upsilon_{2\rho} = -\sum_{n=2}^{\infty} [B_n \gamma_n^{(1)}(r,\theta) + D_n \gamma_n^{(2)}(r,\theta)] + \upsilon_\infty \sum_{m=1}^{\infty} T_m \gamma_m^{(5)}(r,\theta), \tag{25a}$$

$$\upsilon_{2z} = -\sum_{n=2}^{\infty} [B_n \gamma_n^{(3)}(r,\theta) + D_n \gamma_n^{(4)}(r,\theta)] + \upsilon_\infty \sum_{m=1}^{\infty} T_m \gamma_m^{(6)}(r,\theta), \tag{25b}$$

where the definition of functions $\gamma_n^{(i)}(r, \theta)$ for $i = 1$, 2, 3, 4, 5 and 6 is given by Eqs. A11–A16.

The only boundary condition that remains to be satisfied is that on the sphere surface. Substituting Eqs. 6–9 and 25 into Eq. 18a one obtains

$$\sum_{n=2}^{\infty} [B_n \gamma_n^{(1)}(a,\theta) + D_n \gamma_n^{(2)}(a,\theta)] = \upsilon_\infty \sum_{m=1}^{\infty} T_m \gamma_m^{(5)}(a,\theta) - U_0 \sum_{m=1}^{\infty} T_m \gamma_m^{(7)}(a,\theta), \tag{26a}$$

$$\sum_{n=2}^{\infty} [B_n \gamma_n^{(3)}(a,\theta) + D_n \gamma_n^{(4)}(a,\theta)] = \upsilon_\infty \sum_{m=1}^{\infty} T_m \gamma_m^{(6)}(a,\theta) - U_0 \sum_{m=1}^{\infty} T_m \gamma_m^{(8)}(a,\theta) + U_0, \tag{26b}$$

where $\gamma_m^{(7)}(r, \theta)$ and $\gamma_m^{(8)}(r, \theta)$ are defined by Eqs. A17 and A18, and $U_0 = \epsilon\zeta_p E_\infty/4\pi\eta$, which is the electrophoretic velocity of the particle when the pore is not present. The first M coefficients T_m have been determined through the proce-

dure given in the previous subsection. The relations Eqs. 26a and 26b can be satisfied by utilizing the collocation technique presented for the solution of the electrical potential field. At the particle surface, Eqs. 26a and 26b are applied at N discrete points (values of θ between 0 and $\pi/2$) and the infinite series in Eqs. 25 are truncated after N or M terms. This generates a set of $2N$ linear algebraic equations for the $2N$ unknown coefficients B_n and D_n. The fluid velocity field is completely obtained once these coefficients are solved. Note that the definite integrals in Eq. 26 after the substitution of Eqs. A11–A18 must be performed numerically.

The drag force exerted by the fluid on the spherical boundary $r = a$ can be determined from (Happel and Brenner, 1983)

$$F_2 = \eta\pi \int_0^{\pi} r^3 \sin^3\theta \frac{\partial}{\partial r}\left(\frac{E^2\Psi_2}{r^2\sin^2\theta}\right) r d\theta. \tag{27}$$

Substitution of Eqs. 19–21 into the above integral and application of the orthogonality properties of the Gegenbauer polynomials result in the simple relation

$$F_2 = 4\pi\eta D_2. \tag{28}$$

Equation 28 shows that only the coefficient D_2 contributes to the drag force exerted on the particle.

Derivation of the particle velocity

Since the net force acting on the electrophoretic particle must vanish, one has

$$F_1 + F_2 = 0. \tag{29}$$

Substitution of the individual forces given by Eqs. 17 and 28 yields the particle velocity

$$U = v_\infty + \frac{2D_2}{3a\alpha}. \tag{30}$$

Due to the existence of the electroosmotic velocity v_∞ far from the particle, the direction of the movement of the particle is determined by the difference in zeta potentials $\zeta_p - \zeta_w$.

Results and Discussion

The solutions for the electrophoretic motion of a nonconducting sphere along the axis of a circular cylindrical pore, obtained by using the collocation technique described in the previous section, will be presented in this section. These collocation results will be compared with the asymptotic solution developed by Keh and Anderson (1985). The system of linear algebraic equations to be solved for coefficients T_m is constructed from Eq. 11, while that for B_n and D_n is composed of Eq. 26. All the numerical integrations to evaluate functions α_m and $\gamma_n^{(i)}$ were done by the 180-point Gauss-Laguerre quadrature. The numerical calculations were performed by using a DEC 3000/600 workstation.

When specifying the points along the quarter-circular generating arc of the sphere where the boundary conditions are to be exactly satisfied, the first point that should be chosen is $\theta = \pi/2$, since this point defines the projected area of the sphere normal to the direction of motion and controls the gap between the sphere and the pore wall. In addition, the point $\theta = 0$ is also important. However, an examination of the systems of linear algebraic Eqs. 11 and 26 shows that the matrix equations become singular if these points are used. To overcome this difficulty, these points are replaced by closely adjacent points, i.e., $\theta = \delta$ and $\theta = \pi/2 - \delta$. Additional points along the boundary are selected to divide the quarter-arc of the sphere into equal segments. The optimum value of δ in this work is found to be 0.1°, with which the numerical results of the particle velocity can converge to at least five significant digits for any ratios of particle-to-pore radii a/b up to 0.999.

Laying the boundary effect of viscous retardation aside, the electrophoretic velocity of a particle is determined by the magnitude of the electrical potential gradient at the particle surface. A meridian sketch of the electric field lines (with a constant electric field function V for each) and the equipotential lines around a dielectric sphere undergoing electrophoresis in an unbounded fluid is exhibited in Figure 2a. The distortion of these contours due to the presence of the

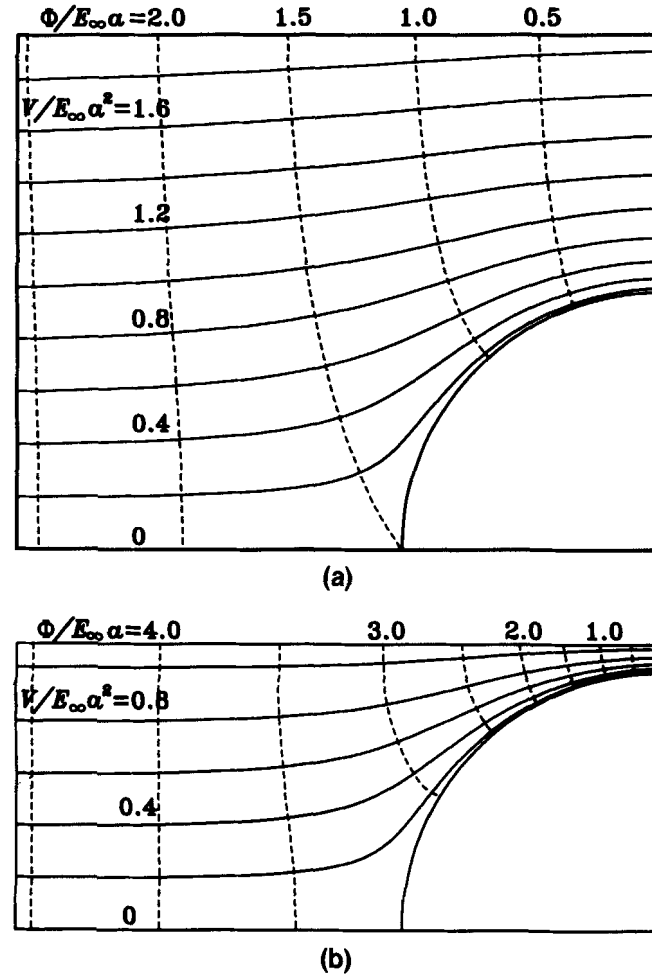

Figure 2. Electric field (——) and equipotential (---) lines for the electrophoresis of a spherical particle.

(a) Migration in an unbounded medium ($a/b = 0$); (b) migration along the axis of a circular cylindrical pore with $a/b = 0.9$.

pore wall is illustrated in Figure 2b for the case of the ratio of particle-to-pore radii a/b equal to 0.9. Since both the particle and the wall are nonconducting, all current is conducted through the suspending fluid. The equipotential lines intersect the particle and wall surfaces at right angles and the electric field lines in the vicinity of the surfaces are parallel to them. The potential gradients along the surface of a sphere in the pore are larger than the corresponding values of the sphere in an unbounded medium, and the difference increases with the increase of the ratio a/b.

A sketch of the streamline pattern for an infinite fluid surrounding a sphere undergoing electrophoresis was exhibited by Anderson (1986), which shows that the fluid reverses itself and flows in the direction opposite to the movement of the particle. For the electrophoretic motion of a sphere along the axis of a circular cylindrical pore, the stream function for the fluid flow can be evaluated from the combination of Ψ_1 obtained by Leichtberg et al. (1976) and Ψ_2 given by Eqs. 19–21 with coefficients determined by the collocation technique. The streamlines for the situation that the pore wall is neutral ($\zeta_w = 0$) are depicted in Figure 3a for the case of $a/b = 0.8$. It can be seen that the fluid recirculation around the sphere is distorted substantially by the wall. In Figure 3b, the streamline pattern for the translation of a sphere along the axis of a cylindrical pore driven by a body force (such as sedimentation) is also illustrated for a comparison. The stream function for this case is calculated from Ψ_1 only with $U_\infty = 0$.

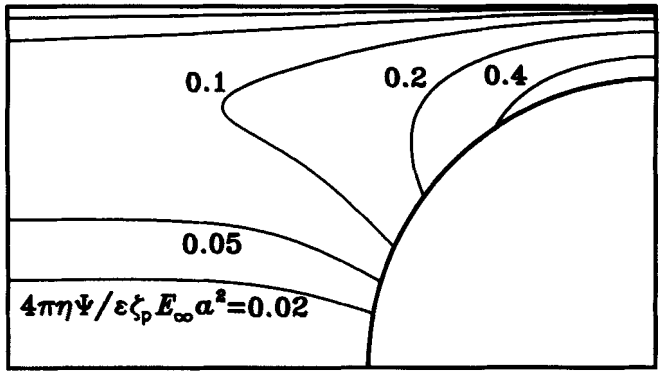

(a)

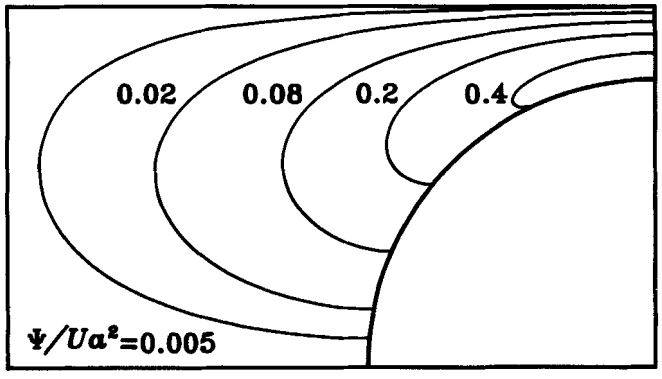

(b)

Figure 3. Streamlines around a spherical particle moving along the axis of a circular cylindrical pore with $a/b = 0.8$.

(a) Electrophoresis (with $\zeta_w = 0$); (b) sedimentation.

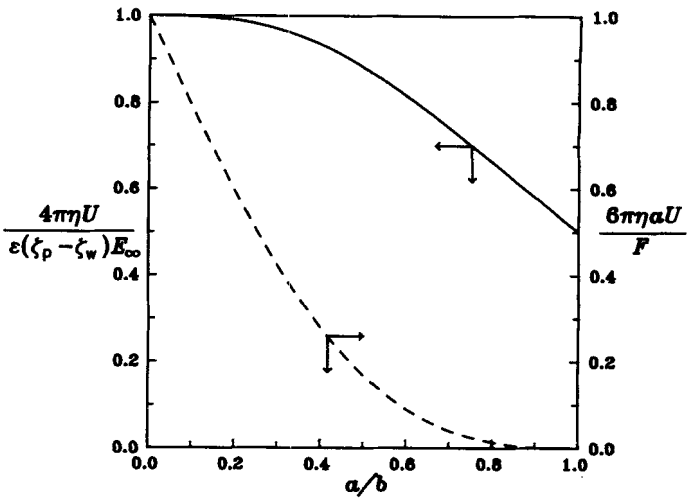

Figure 4. Normalized electrophoretic mobility (——) and Stokes mobility (---) of a spherical particle moving along the axis of a circular cylindrical pore vs. the ratio a/b.

Since the fluid is set motionless far from the particle, a global recirculating flow is observed in Figure 3b.

The collocation solutions of the wall-corrected normalized electrophoretic mobility $[4\pi\eta U/\epsilon(\zeta_p - \zeta_w)E_\infty]$ for a sphere moving along the axis of a cylindrical pore for various values of the ratio of particle-to-pore radii are presented in the first and second columns of Table 1 and depicted by a solid curve in Figure 4. All of the results obtained under this collocation scheme converge to at least five significant figures. The accuracy of the truncation technique is principally a function of the ratio a/b. For the difficult case of $a/b = 0.999$, the numbers of collocation points $M = 72$ and $N = 84$ are sufficiently large to achieve this convergence. Examination of the results shown in Table 1 and Figure 4 reveals that the electrophoretic mobility of the particle is a monotonic decreasing function of a/b. These results indicate that the wall effect of hydrodynamic resistance on the particle in the pore is overriding in the competition with the wall effect of electrostatic

Table 1. Normalized Electrophoretic Mobility for the Motion of a Sphere Along the Axis of a Cylindrical Pore*

	$4\pi\eta U/[\epsilon(\zeta_p - \zeta_w)E_\infty]$	
a/b	Exact Solution	Asymptotic Solution
0.1	0.99873	0.99873
0.2	0.99022	0.99022
0.3	0.96899	0.96903
0.4	0.93228	0.93266
0.5	0.88018	0.88197
0.6	0.81500	0.82089
0.7	0.74041	0.75537
0.8	0.66057	0.69154
0.9	0.57938	0.63323
0.95	0.53931	0.60591
0.99	0.50783	0.58417
0.995	0.50400	0.58142
0.999	0.50177	0.57921

*Computed from the exact boundary-collocation solution and the asymptotic method-of-reflection solution.

enhancement. On the contrary, when the particle is undergoing electrophoresis parallel to a dielectric plane wall, the competition between these two opposite forces shows that the net wall effect can speed up the movement of the particle (Keh and Chen, 1988). An explanation of this consequence might be that fluid must be squeezed through the gap between the cylinder and the sphere undergoing axial electrophoresis; this is unlike the case of the sphere migrating parallel to the plane wall, where fluid can more easily go over the top of the sphere and not through the gap reducing the retarding effect of the fluid. Note that, the electrophoretic mobility of a large sphere in a small pore with $a/b = 0.999$ will still have about half of the value with the pore wall being far away from the particle.

Using a method of reflections, Keh and Anderson (1985) obtained the following power series expression in $\lambda (= a/b)$ for the same electrophoretic motion as that considered in this work

$$\frac{4\pi\eta U}{\epsilon(\zeta_p - \zeta_w)E_\infty} = 1 - 1.28987\lambda^3 + 1.89632\lambda^5 - 1.02780\lambda^6 + O(\lambda^8). \quad (31)$$

The values of the normalized electrophoretic mobility calculated from this asymptotic solution, with $O(\lambda^8)$ term neglected, are also listed in Table 1 for comparison. It can be seen that the asymptotic formula of Eq. 31 from the method of reflections agrees very well with the exact results as long as $\lambda \leq 0.7$; the error in this case will be less than 2.1%. However, accuracy of Eq. 31 begins to deteriorate, as expected, when the relative spacing between the particle and the pore wall becomes small (say, $\lambda \geq 0.8$). The formula of Eq. 31 always overestimates the electrophoretic velocity of the particle.

The collocation results in Table 1 can be compared with the following expression for the electrophoretic velocity of a charged sphere with a thin double layer situated at the center of an uncharged spherical cavity ($\zeta_w = 0$) analytically developed by Zydney (1995)

$$\frac{4\pi\eta U}{\epsilon\zeta_p E_\infty} = \frac{2 - 5\lambda^3 + 3\lambda^5}{2(1-\lambda^3)(1-\lambda^5)}, \quad (32)$$

where λ is now the ratio of the particle-to-cavity radii. This dimensionless electrophoretic mobility decreases monotonically from unity at $\lambda = 0$ to one-half as $\lambda \to 1$. The boundary effects on electrophoresis in cylindrical and spherical pores are quite similar, with the hindrance in the cylindrical pore being somewhat smaller than that in the spherical cavity at all λ as expected. The excellent agreement between the numerical values for the dimensionless mobility at fixed values of λ is striking, with the results being within 2.6%. The similarity in the hindering effects in these pore geometries reflects the fact that the deformation of the electric field and the viscous retardation in the cylindrical pore geometry are greatest at the point of closest approach of the sphere to the pore wall, with the geometry of this region being analogous to that of a sphere in the spherical cavity (Zydney, 1995).

For the motion of a sphere on which a constant body force F such as gravity is exerted along the axis of a cylindrical pore, the particle velocity was obtained in a power series of λ up to $O(\lambda^{10})$ (Happel and Brenner, 1983) and by using the boundary-collocation technique (Leichtberg et al., 1976). The Stokes-law correction for various values of λ has been computed, and the collocation results of factor $6\pi\eta aU/F\ (= 1/\alpha)$ are plotted by a dashed curve in Figure 4 for comparison. Obviously, the wall effect on electrophoresis is much weaker than that on a sedimenting particle.

Conclusion

In this work, the solution for the electrophoretic motion of a colloidal sphere along the axis of a circular cylindrical pore in the limit of $\kappa a \to \infty$ has been obtained. For an open system with no pressure gradients far from the particle, a net electro-osmotic flow is allowed to occur and the direction of particle motion is determined by the difference in zeta potentials $\zeta_p - \zeta_w$. Laying this influence of electro-osmosis aside, the wall effect on electrophoresis is to slow down the particle velocity for various separation distances (up to $a/b = 0.999$). This behavior reflects the predominance of the hydrodynamic retardation of the pore wall on the particle migration over the electrophoresis enhancement due to the electrostatic interaction between the particle and the wall. On the other hand, the electrophoretic velocity of a dielectric sphere can be increased significantly by a lateral plane wall when the gap spacing is small (Keh and Chen, 1988).

It has been found that the electrophoretic mobility of a sphere in a pore is a monotonic decreasing function of a/b and its value for the case of $a/b = 0.999$ is about half of that for the case of $a/b = 0$. This is in sharp contrast to the results for the corresponding sedimentation problem in which the scaled particle velocity goes to zero in the limit $a/b \to 1$. This behavior was also seen in the work by Zydney (1995) on the electrophoresis of a sphere in a concentric spherical cavity. It might be of interest to actually calculate the value of the electrophoretic mobility of a colloidal sphere along the axis of a cylindrical pore for the limiting situation of $a/b = 1$ (still with the assumption of thin double layers). This calculation may be made by utilizing a lubrication theory (Lighthill, 1968; Hochmuth and Sutera, 1970) or a singular perturbation technique (Bungay and Brenner, 1973), which was used successfully in the treatment of the Stokes motion of a large sphere in the axial direction of a long tube.

Acknowledgment

This research was supported by the National Science Council of the Republic of China under grant NSC83-0402-E002-067.

Notation

a = particle radius, m
$A_n^{(i)}(\omega)$ = functions defined by Eq. 24 or Eqs. A6–A10
b = pore radius, m
E_∞, E_∞ = uniform applied electric field, V·m^{-1}
F_1, F_2 = drag forces exerted on the particle for two subproblems, N
I_n = modified Bessel functions of the first kind
K_n = modified Bessel functions of the second kind
M, N = number of collocation points on the particle surface
r, θ, ϕ = spherical coordinates
U, U = particle velocity, m·s^{-1}

U_0, U_0 = particle velocity in an unbounded medium, $m \cdot s^{-1}$
v = fluid velocity field, $m \cdot s^{-1}$
v_ρ, v_z = components of v in cylindrical coordinates, $m \cdot s^{-1}$
$v_\infty = -\epsilon\zeta_w E_\infty / 4\pi\eta$, $m \cdot s^{-1}$
z, ρ, ϕ = cylindrical coordinates

Greek letters

α_m = functions of r and θ defined by Eq. 12
$\beta_n^{(i)}$ = functions of ρ and z defined by Eqs. A1–A5
$\gamma_n^{(i)}$ = functions of r and θ defined by Eqs. A11–A18
$\epsilon/4\pi$ = fluid permittivity, $C^2 \cdot J^{-1} \cdot m^{-1}$
ζ_p = zeta potential of the particle, V
ζ_w = zeta potential of the pore wall, V
η = fluid viscosity, $kg \cdot m^{-1} \cdot s^{-1}$
θ, ϕ, r = spherical coordinates
κ = reciprocal Debye screening length, m^{-1}
ρ, ϕ, z = cylindrical coordinates
Φ = electrical potential field, V
Ψ = stream function, $m^3 \cdot s^{-1}$
Ψ_1, Ψ_2 = stream functions for two subproblems, $m^3 \cdot s^{-1}$

Literature Cited

Anderson, J. L., "Transport Mechanisms of Biological Colloids," *Ann. N. Y. Acad. Sci.*, **469** (Biochem. Eng. 4), 166 (1986).
Anderson, J. L., "Colloid Transport by Interfacial Forces," *Ann. Rev. Fluid Mech.*, **21**, 61 (1989).
Bungay, P. M., and H. Brenner, "The Motion of a Closely-Fitting Sphere in a Fluid-Filled Tube," *Int. J. Multiphase Flow*, **1**, 25 (1973).
Ewing, A. G., R. A. Wallingford, and T. M. Olefirowicz, "Capillary Electrophoresis," *Anal. Chem.*, **61**, 292A (1989).
Haber, S., and L. Gal-Or, "Deep Electrophoretic Penetration and Deposition of Ceramic Particles inside Porous Substrates: I. Analytical Model," *J. Electrochem. Soc.*, **139**, 1071 (1992).
Haberman, W. L., and R. M. Sayre, "Motion of Rigid and Fluid Spheres in Stationary and Moving Liquids Inside Cylindrical Tubes," David Taylor Model Basin Report No. 1143, U.S. Navy Dept. (1958).
Happel, J., and H. Brenner, *Low Reynolds Number Hydrodynamics*, Martinus Nijhoff, The Netherlands (1983).
Hochmuth, R. M., and S. P. Sutera, "Spherical Caps in Low Reynolds-Number Tube Flow," *Chem. Eng. Sci.*, **25**, 593 (1970).
Huner, R. J., *Foundations of Colloid Science*, Vol. II, Clarendon Press, Oxford, p. 808 (1989).
Jorgenson, J. W., "Electrophoresis," *Anal. Chem.*, **58**, 743A (1986).
Keh, H. J., and J. L. Anderson, "Boundary Effects on Electrophoretic Motion of Colloidal Spheres," *J. Fluid Mech.*, **153**, 417 (1985).
Keh, H. J., and S. B. Chen, "Electrophoresis of a Colloidal Sphere Parallel to a Dielectric Plane," *J. Fluid Mech.*, **194**, 377 (1988).
Keh, H. J., and L. C. Lien, "Electrophoresis of a Colloidal Sphere Along the Axis of a Circular Orifice or a Circular Disk," *J. Fluid Mech.*, **224**, 305 (1991).
Leichtberg, S., R. Pfeffer, and S. Weinbaum, "Stokes Flow Past Finite Coaxial Clusters of Spheres in a Circular Cylinder," *Int. J. Multiphase Flow*, **3**, 147 (1976).
Lighthill, M. J., "Pressure-Forcing of Tightly Fitting Pellets Along Fluid-Filled Elastic Tubes," *J. Fluid Mech.*, **34**, 113 (1968).
Morrison, F. A., "Electrophoresis of a Particle of Arbitrary Shape," *J. Colloid Interf. Sci.*, **34**, 210 (1970).
Morrison, F. A., and J. J. Stukel, "Electrophoresis of an Insulating Sphere Normal to a Conducting Plane," *J. Colloid Interf. Sci.*, **33**, 88 (1970).
O'Brien, R. W., and D. N. Ward, "The Electrophoresis of a Spheroid with a Thin Double Layer," *J. Colloid Interf. Sci.*, **121**, 402 (1988).
Smith, F. G., and W. M. Deen, "Electrostatic Double-Layer Interactions for Spherical Colloids in Cylindrical Pores," *J. Colloid Interf. Sci.*, **78**, 444 (1980).
Smith, F. G., and W. M. Deen, "Electrostatic Effects on the Partitioning of Spherical Colloids between Dilute Bulk Solution and Cylindrical Pore," *J. Colloid Interf. Sci.*, **91**, 571 (1983).
Zydney, A. L., "Boundary Effects on the Electrophoretic Motion of a Charged Particle in a Spherical Cavity," *J. Colloid Interf. Sci.*, **169**, 476 (1995).

Appendix

For completeness the definitions of some functions in Eqs. 22–26 are listed here.

$$\beta_n^{(1)}(\rho,z) = \frac{n+1}{\rho(\rho^2+z^2)^{n/2}} G_{n+1}^{-1/2}\left[\frac{z}{(\rho^2+z^2)^{1/2}}\right] \quad \text{(A1)}$$

$$\beta_n^{(2)}(\rho,z) = \frac{n+1}{\rho(\rho^2+z^2)^{(n-2)/2}} G_{n+1}^{-1/2}\left[\frac{z}{(\rho^2+z^2)^{1/2}}\right] - \frac{2z}{\rho(\rho^2+z^2)^{(n-1)/2}} G_n^{-1/2}\left[\frac{z}{(\rho^2+z^2)^{1/2}}\right] \quad \text{(A2)}$$

$$\beta_n^{(3)}(\rho,z) = \frac{1}{(\rho^2+z^2)^{(n+1)/2}} P_n\left[\frac{z}{(\rho^2+z^2)^{1/2}}\right] \quad \text{(A3)}$$

$$\beta_n^{(4)}(\rho,z) = \frac{2}{(\rho^2+z^2)^{(n-1)/2}} G_n^{-1/2}\left[\frac{z}{(\rho^2+z^2)^{1/2}}\right] + \frac{1}{(\rho^2+z^2)^{(n-1)/2}} P_n\left[\frac{z}{(\rho^2+z^2)^{1/2}}\right] \quad \text{(A4)}$$

$$\beta_m^{(5)}(\rho,z) = (-1)^{(m-1)/2}\frac{2}{\pi m!}\int_0^\infty \omega^{m+1}\frac{K_1(b\omega)}{I_1(b\omega)} \times I_0(\omega\rho)\cos(\omega z)\,d\omega - \frac{m+1}{(\rho^2+z^2)^{(m+2)/2}} P_{m+1}\left[\frac{z}{(\rho^2+z^2)^{1/2}}\right], \quad \text{(A5)}$$

where m is odd and n is even in Eqs. 22, 23, 25 and 26.

$$A_n^{(1)}(\omega) = -(-1)^{n/2}\frac{2\omega^n}{\pi n!}K_1(b\omega) \quad \text{(A6)}$$

$$A_n^{(2)}(\omega) = -(-1)^{n/2}\frac{2\omega^{n-2}}{\pi n!}[(2n-3)b\omega K_0(b\omega) - (n-2)(n-3)K_1(b\omega)] \quad \text{(A7)}$$

$$A_n^{(3)}(\omega) = (-1)^{n/2}\frac{2\omega^n}{\pi n!}K_0(b\omega) \quad \text{(A8)}$$

$$A_n^{(4)}(\omega) = -(-1)^{n/2}\frac{2\omega^{n-2}}{\pi n!}[n(n-1)K_0(b\omega) - (2n-3)b\omega K_1(b\omega)] \quad \text{(A9)}$$

$$A_m^{(5)}(\omega) = (-1)^{(m-1)/2}\frac{2\omega^{m+1}}{\pi m!}\left[K_0(b\omega) + \frac{K_1(b\omega)}{I_1(b\omega)}I_0(b\omega)\right] \quad \text{(A10)}$$

where I_n and K_n are the modified Bessel functions of the first and second kinds, respectively, of order n.

$$\gamma_n^{(1)}(r,\theta) = r^{-n-1}\frac{n+1}{\sin\theta}G_n^{-1/2}(\cos\theta) + \int_0^\infty \frac{1}{\Delta}\{-[A_n^{(1)}(\omega) - \Omega A_n^{(3)}(\omega)]\omega r\sin\theta I_0(\omega r\sin\theta) + [(2+b\omega\Omega)A_n^{(1)}(\omega) - b\omega A_n^{(3)}(\omega)]I_1(\omega r\sin\theta)\}\sin(\omega r\cos\theta)d\omega \quad \text{(A11)}$$

$$\gamma_n^{(2)}(r,\theta) = r^{-n+1}\left[\frac{n+1}{\sin\theta}G_{n+1}^{-1/2}(\cos\theta) - \frac{2}{\tan\theta}G_n^{-1/2}(\cos\theta)\right] + \int_0^\infty \frac{1}{\Delta}\{-[A_n^{(2)}(\omega) - \Omega A_n^{(4)}(\omega)]\omega r\sin\theta I_0(\omega r\sin\theta) + [(2+b\omega\Omega)A_n^{(2)}(\omega) - b\omega A_n^{(4)}(\omega)]I_1(\omega r\sin\theta)\} \times \sin(\omega r\cos\theta)d\omega \quad \text{(A12)}$$

$$\gamma_n^{(3)}(r,\theta) = r^{-n-1}P_n(\cos\theta) + \int_0^\infty \frac{1}{\Delta}\{[b\omega\Omega A_n^{(1)}(\omega) + (2\Omega - b\omega)A_n^{(3)}(\omega)]I_0(\omega r\sin\theta) - [(A_n^{(1)}(\omega) - \Omega A_n^{(3)}(\omega)]I_1(\omega r\sin\theta)\}\cos(\omega r\cos\theta)d\omega \quad \text{(A13)}$$

$$\gamma_n^{(4)}(r,\theta) = r^{-n+1}[P_n(\cos\theta) + 2G_n^{-1/2}(\cos\theta)] + \int_0^\infty \frac{1}{\Delta}\{[b\omega\Omega A_n^{(2)}(\omega) + (2\Omega - b\omega)A_n^{(4)}(\omega)]I_0(\omega r\sin\theta) - [A_n^{(2)}(\omega) - \Omega A_n^{(4)}(\omega)]I_1(\omega r\sin\theta)\}\cos(\omega r\cos\theta)d\omega \quad \text{(A14)}$$

$$\gamma_m^{(5)}(r,\theta) = \int_0^\infty \frac{1}{\Delta}A_m^{(5)}(\omega)[\Omega\omega r\sin\theta I_0(\omega r\sin\theta) - b\omega I_1(\omega r\sin\theta)]\sin(\omega r\cos\theta)d\omega \quad \text{(A15)}$$

$$\gamma_m^{(6)}(r,\theta) = \int_0^\infty \frac{1}{\Delta}A_m^{(5)}(\omega)[(2\Omega - b\omega)I_0(\omega r\sin\theta) + \Omega\omega r\sin\theta I_1(\omega r\sin\theta)]\cos(\omega r\cos\theta)d\omega \quad \text{(A16)}$$

$$\gamma_m^{(7)}(r,\theta) = (-1)^{(m-1)/2}\frac{2}{\pi m!}\int_0^\infty \omega^{m+1}\frac{K_1(b\omega)}{I_1(b\omega)} \times I_1(\omega r\sin\theta)\sin(\omega r\cos\theta)d\omega - (m+1)(m+2)r^{-(m+2)}\frac{G_{n+2}^{-1/2}(\cos\theta)}{\sin\theta} \quad \text{(A17)}$$

$$\gamma_m^{(8)}(r,\theta) = (-1)^{(m-1)/2}\frac{2}{\pi m!}\int_0^\infty \omega^{m+1}\frac{K_1(b\omega)}{I_1(b\omega)} \times I_0(\omega r\sin\theta)\cos(\omega r\cos\theta)d\omega - (m+1)r^{-(m+2)}P_{m+1}(\cos\theta) \quad \text{(A18)}$$

where

$$\Delta = b\omega(1-\Omega^2)I_0(b\omega) - 2I_1(b\omega) \quad \text{(A19)}$$

$$\Omega = \frac{I_1(b\omega)}{I_0(b\omega)}. \quad \text{(A20)}$$

Manuscript received May 8, 1995, and revision received Aug. 7, 1995.